

# Advanced 3D Robot Simulation for Flexible Interactive Manual Robot Guidance—An eRobotics Approach

Eric Guiffo Kaigom<sup>\*</sup> and Jürgen Roßmann

Institute for Man-Machine  
Interaction  
RWTH University  
Aachen, Germany

## ABSTRACT

*Manual robot guidance is an intuitive approach to teach robots with human's skills in the loop. It is particularly useful to manufacturers because of the high flexibility and low programming efforts. However, manual robot guidance requires compliance control that is generally not available in industrial robots. We address this issue with a simulation-based approach. The dynamics of the robot are replicated and its motion is controlled on the simulator, which is enriched with a joint admittance controller driven in real time with external joint torques sensed during interaction with the physical robot. We then virtually transfer the admittance capability by sending back the simulated compliant joint position to the real robot to enable manual guidance. Experimental case studies are provided to illustrate the practical performance and usefulness of the proposed smooth bidirectional transition between 3D simulation and reality, as pursued by eRobotics to address complex issues in industrial automation.*

## 1. INTRODUCTION

Current trends in service robotics show a significant enhancement of safety and performance of robot manipulators. Some recently developed light-weight robots (see Figure 1) have been endowed with the capability to accommodate undesired external forces. In contrast to industrial robot traditionally kept away from humans, such human-friendly robots are particularly well-suited to dynamic work cells, in which a close physical interaction between humans and robots improves and streamlines task achievement. This way, manufacturers can take advantage of human skills in the loop in order to quickly adapt their production to heterogeneous demands from the market.

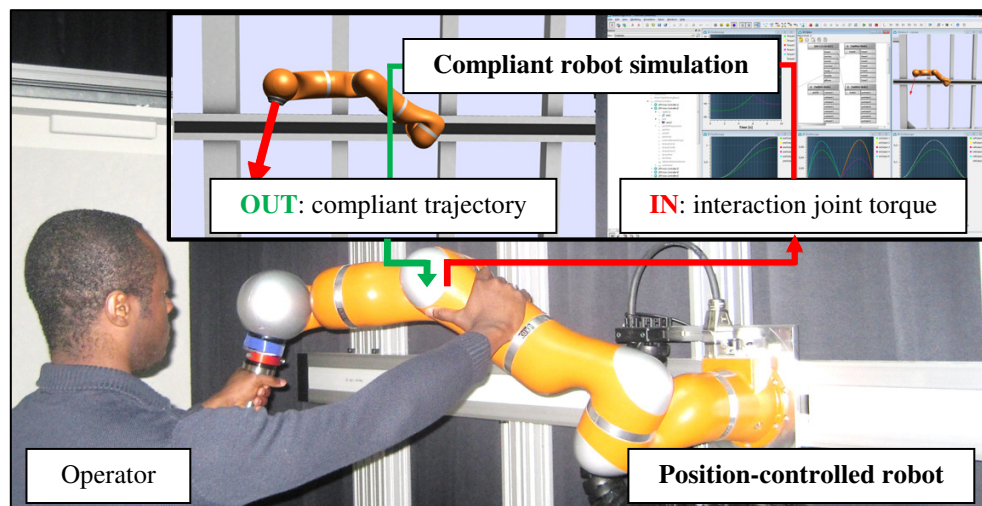


Figure 1. 3D simulation-based full-body robot manual guidance.

---

<sup>\*</sup> Corresponding author: Tel.: (0049) 241-8026101; Fax: (0049) 214-8022308; E-mail: kaigom@mmi.rwth-aachen.de

On the other side, external forces can be apprehended as means of communication between an operator and the robot with the purpose of guiding the robot manually (see Figure 1). Once the robot compliance is appropriately programmed, even novice users can easily lead the robot along a desired path in order to achieve tasks that would otherwise require advanced programming skills and preliminary collision avoidance check. Besides time- and cost-saving benefits, this intuitive and flexible approach to guide a robot has been shown to perform in many applications, including grasping tasks, better than the automated counterpart [1].

Nonetheless, compliance control required for manual guidance is not available on standard robots. During the last years, few approaches have been proposed to cope with this issue. In [2], the motor current feedback is utilized to estimate external interaction forces. A Cartesian admittance controller is then implemented to accommodate for external forces. A similar approach has been proposed in [3], where the magnitude and direction of the exerted external force are estimated. A sensor-based Cartesian admittance control has been used for physical robot guidance in [4]. External forces exerted on the tool center point (TCP) of the robot are measured to drive an admittance controller that accommodates for the motion commanded by the operator.

In many situations, however, an operator may need to interact with links other than the end-link in order for instance to explicitly modify the robot posture for avoiding a collision or reducing the effective mass (EM) of the TCP. The latter aspect is important for mitigating the impulsive force in case of collision. While human perception and adaptability skills are useful for collision-free guidance, computer simulation is more suitable for estimating the effective mass of the TCP along a given direction.

Following the research objectives of eRobotics [5] that draws upon simulation-driven engineering to support the lifecycle and to extend the functionalities of complex systems in robotics and automation (see Figure 2), the present work combines robot modelling and control with the strengths of virtual reality to provide a flexible approach for physical interactive guidance of a real position-controlled redundant robot manipulator. In this respect, our contribution highlights how the symbiosis between virtual reality and real robotic systems fosters and augments the effectiveness, practicability and applicability of human-robot interaction in industrial manufacturing.

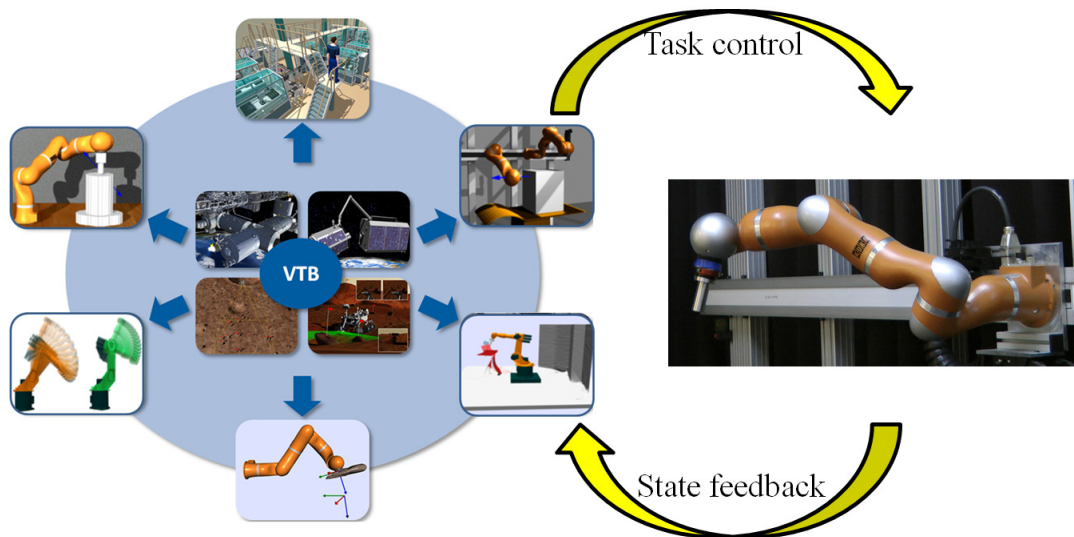


Figure 2. eRobotics extends and strengthens the Virtual Test-Bed (VTB) idea from space robotics in order to address issues related to robotic automation. It strives to maximize the added value that results from introducing advanced 3D simulation into industrial applications. A prominent goal is to extend hardware functionalities through simulation-based control.

In order to achieve these objectives, we first capture and replicate the robot dynamics, in which we are interested, on a comprehensive and multipurpose multi-body simulator. Then, dynamic joint admittance control relying upon joint position and torque control is shifted onto a simulator that serves as virtual robotic test-bed (VTB) as well. The simulated joint admittance controller is driven with real external joint torques estimated by the real robotic system when the operator touches the robot. With the aim of reducing the amount of robot resistance felt by the operator during physical interaction, the joint admittance parameters are adapted in a simple fashion. The resulting simulated compliant joint trajectories are fed back in real-time into the real robot control unit to achieve the intended physical robot

guidance. In contrast to the approach in [4] that focuses attention on interactions with the TCP, the guidance in this work is possible by touching any link of the robot manipulator. This enables a better and explicit reachability of different postures for task achievement as well as optimization purposes.

The remainder of this paper is structured as follows. We briefly present in section 2 the eRobotics concept on which the ideas developed in this work are based. In section 3, we couple on the simulator two modelling paradigms in order, on the one side, to simulate the robot and its environment, and on the other side, to realize a torque based position control of the robot. We capture the key properties of the robot in which we are interested to endow the simulated robot in section 4 with a robust, highly modular and adaptable joint admittance control. In addition, the adaption of the compliance is presented. We proceed in section 5 with practical case studies. Single joint motions, full-body as well as TCP-centered guidance carried out on a physical 7 degrees of freedom (DoF) robot manipulator are presented. We illustrate the intuitiveness, usefulness, flexibility and versatility of the approach with respect to different potential practical applications in the industrial manufacturing sector. Finally, section 6 is for discussion and conclusion.

## 2. EROBOTICS

3D simulation technology is widespread in industry today e.g. for planning tasks in robot-assisted manufacturing. This increases flexibility, productivity and competitiveness. However, there is still a considerable gap between the current outcomes driven by simulation and its high potential in industry as direct source of added value. This is partly due to the conceptual limitations of the simulation approach (e.g. dedicated single process simulation) that inhibit the functionality extension of traditional hardware, and the lack of versatility to swiftly adapt to recent advances in robotics and automation such as safe close human-robot interaction.

As shown in Figure 2, the eRobotics concept [5] addresses these issues by strengthening and extending the virtual test-bed idea from space robotics [6] in order to provide a multipurpose, holistic, versatile and collaborative 3D simulation platform. It then broadens this know-how to diverse research and application areas of robotics automation in order to support the entire lifecycle of products, while paving the way for new technologies [7]. A prominent objective of eRobotics that particularly motivates the present work is to maximize the benefit that robotic hardware and algorithm development can draw from the symbiosis between robotics and virtual reality techniques [8].

## 3. ROBOT AND ENVIRONMENT MODELING

In this section, the coupling of two modeling techniques termed as the maximal (i.e. Cartesian) and reduced (i.e. joint variables) coordinates scheme is outlined. As depicted in Figure 3, the simulation of the robot and its environment as

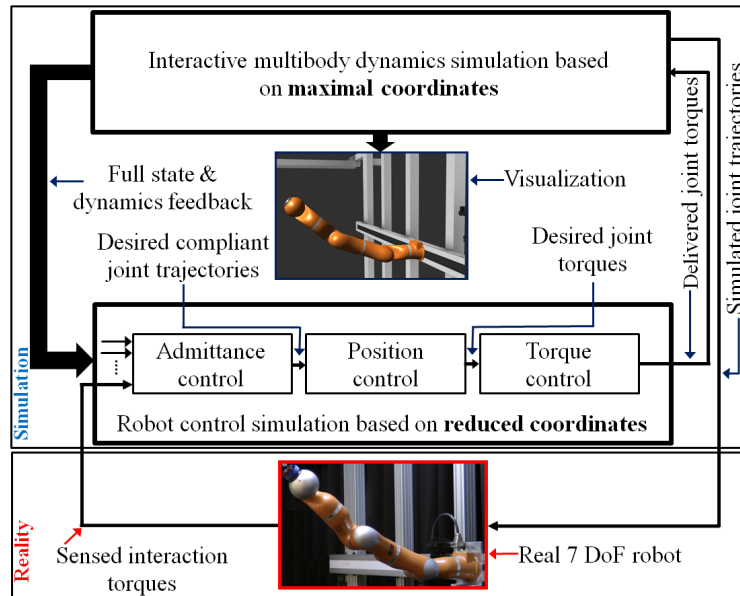


Figure 3. Coupling modeling paradigms for context-independent modeling and simulated robot control.

multi-body systems is based upon the former technique. The latter one is used to control the robot dynamics.

### 3.1. INTERACTIVE MULTI-BODY DYNAMICS SIMULATION

Since special emphasis is placed in this work on a physically accurate, multipurpose and interactive simulation, a vast amount of constraints arises, which range from a revolute joint up to friction and non-penetration requirements. In order to uniformly handle both multi-bodies motion and related constraints, the multi-body modeling and simulation approaches developed in this work combin the second law of Newton and forces that workless enforce constraints by being expressed orthogonally to admissible velocities. The Lagrange multipliers describe the signed magnitude of constraint forces [9]. The equations of motion are arranged in a form that contains the Lagrange multipliers as unknowns with equality (e.g. for a joint) or inequality (e.g. for contacts) constraints. This results in a complementary problem that is solved for the Lagrange multipliers. Once the multipliers are determined, the constraint forces follow immediately and the velocity propagation of the maximal coordinates of each body is found.

### 3.2. ROBOT MODELING FOR CONTROL PURPOSE

Depending on the vector of joint position  $q$  and its time derivatives, the Lagrangian dynamic model of the robot manipulator with  $N$  degrees of freedom is given by

$$M(q)\ddot{q} + C(q, \dot{q}) + G(q) = \tau_{act} + \tau_{ext}. \quad (1)$$

$M$ ,  $C$  and  $G$  are the positive definite inertia matrix, velocity-dependent and gravity terms, respectively.  $\tau_{act}$  and  $\tau_{ext}$  are vectors containing the joint actuation and external torques. The vector  $\tau_{ext}$  results from external forces acting on the links of the robot. In order to compute this vector, external forces are first transformed into an equivalent force and moment acting on the center of mass of the related link by using the Poinot's theorem. Then, the transposed of the Jacobi matrix that transforms the joint velocities in links linear and angular velocities is formed. The robot statics are finally invoked to transform the equivalent force and moment over the transposed Jacobi matrix into  $\tau_{ext}$ .

On the other side,  $\tau_{act}$  is furnished by the actuation module, which includes the motor and structural flexibility. In this work, it is assumed that the current control is fast enough, and therefore, neglected. However, the rotor dynamics and structural flexibility are taken into account by considering the joint inertia  $J_m$  as well as stiffness  $K_m$ . Therefore, the motor torque is the sum of the torque necessary to overcome the shaft dynamics and the transmitted torque  $\tau_{act}$  which is in turn equal to the position difference between the motor and joint position weighted by  $K_m$ .

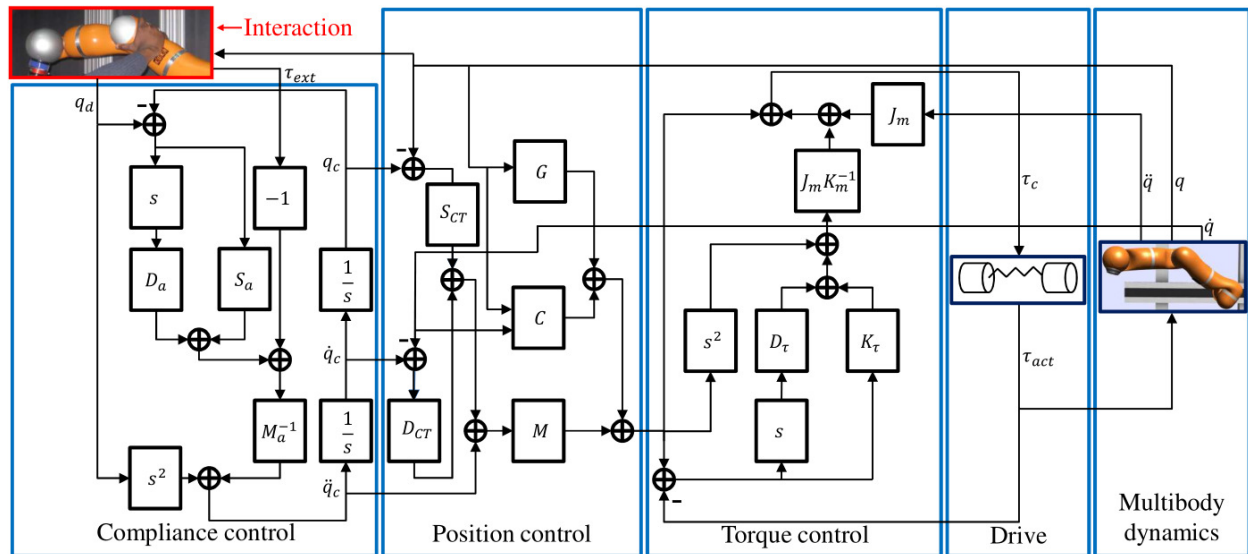


Figure 4. The developed multi-stage joint admittance control simulation scheme.

As illustrated in Figure 4, it is worth to note that the output of the simulated admittance controller (i.e. the desired compliant joint trajectories) presented in the next section is not fed back into the real robot controller. Instead, the input of the latter are the current joint positions of the dynamically simulated and position-controlled robot that acts as a surrogate of the real position-controlled robot *virtually* endowed with joint admittance on the simulator. This capability

is then transferred to the real robot by sending back the *simulated* compliant joint trajectories to the controller of the real position-controlled robot.

#### 4. JOINT ADMITTANCE CONTROL FOR GUIDANCE

When an external joint torque is sensed, a compliant trajectory is generated by the admittance controller. Then, joint position and motor torque control modules are used for tracking the compliant trajectory. In this section, this three-stage control approach is first outlined. Afterwards, the focus is put on the adaptation of compliance parameters to intuitively decrease the amount of robot resistance felt by the operator during physical guidance.

##### 4.1. COMPLIANT TRAJECTORY GENERATION

As shown in Figure 5, joint admittance control enforces a mass-damper-spring behavior of a joint as reaction to an external force. The second-order relationship between torque and position is given by:

$$\begin{aligned}\tau_{ext} &= m_a \ddot{e}_q + d_a \dot{e}_q + s_a e_q, \\ e_q &= q_d - q_c.\end{aligned}\quad (2)$$

In equation (2),  $m_a$ ,  $d_a$ ,  $s_a$ , and  $q_d$  are the desired inertia, damping, stiffness values of the joint contained in the diagonal matrix  $M_a$ ,  $D_a$ , and  $S_a$  (see Figure 4) and the desired joint position. In order to extract the compliant trajectory  $q_c(t)$  at any point of time, equation (2) can be reformulated as a non-homogenous linear equation, whose system matrices contain the joint compliance coefficients. The time continuous compliant trajectory which is the solution of this problem depends on the matrix exponential, which is computed by using the eigenvalues of the system matrix. As we are concerned with computer simulation, a time discrete solution is elaborated, while assuming that the external torques and admittance parameters remain constant between two simulation steps. As a result, the compliant trajectory is fully computed up to acceleration level and fed into the position controller as input (see Figure 4).

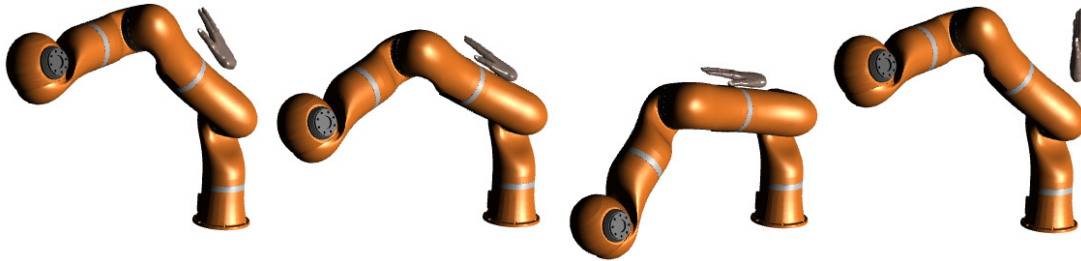


Figure 5. 3D simulated interaction scenario with joint admittance control. From left to right: The hand touches the robot and induces external joint torques. The admittance controller tracks the compliant trajectory. As soon as there is no contact between the robot and the hand anymore, the robot returns to its initial configuration.

##### 4.2. POSITION CONTROL

At the second stage, the computed torques technique with the diagonal matrices of position and velocity gains  $S_{CT}$  and  $D_{CT}$  is used to command the desired torque for tracking the compliant trajectory (see Figure 4). The terms on the left hand side of (1) are computed on the basis of the dynamics and full state feedback as shown in Figure 3. They depend on the relevant parameters of the targeted real robot that have to be identified. These include the link mass and local inertia, joint friction and flexibility.

##### 4.3. TORQUE CONTROL

The joint torques are furnished at the third stage through a technique originally introduced for the Cartesian impedance control of flexible joint robots that decouples the torque dynamics from the rigid link dynamics [10]. This is particularly useful as it allows different torque-based control techniques to be implemented on flexible joint robots. The key idea is to use acceleration feedback and an appropriately designed auxiliary joint torque to enforce an asymptotic stable torque error dynamics given in our case by

$$\ddot{e}_\tau + D_\tau \dot{e}_\tau + (K_\tau + K_m J_m^{-1}) e_\tau = 0, \quad (3)$$



where  $e_\tau$  is the torque error. The control gains  $D_\tau$  and  $K_\tau$  are positive definite diagonal matrices, which influence the convergence rate. It is worth noting that acceleration feedback is not a stringent requirement as joint acceleration is available on the simulator.

#### 4.4. ADAPTATION OF ADMITTANCE PARAMETERS

The modification is based upon a simple human intention deduction. In case of vanishing external joint torques, we infer that the operator does not interact with the robot anymore, so the robot has to be decelerated. Thus, the damping and stiffness values increase as an exponential function of time. However, the time constants are set differently. The damping increases significantly faster than the stiffness. By non-vanishing external torques, the human operator interacts with the robot. Therefore the damping and stiffness values decrease. Note that the maximal joint stiffness is chosen comparatively low as we are concerned with free motion.

### 5. EVALUATION

We have carried out several experiments in order to investigate the effectiveness of the proposed manual guidance. The setup shown in Figure 6 consists of a 7 DoF KUKA LWR robot in position control mode. The robotic system estimates external joint torques by contact. The simulator receives external torques and sends compliant joint position commands every 2ms over the Fast Research Interface [5].

#### 5.1. EXPERIMENT 1 - DECREASING THE FELT ROBOT RESISTANCE

At the beginning of this experiment, the robot is fully extended straight ahead on the horizontal plane (see Figure 6). Except for the fourth joint, the stiffness and damping joint values are set very high. The task performed by the operator

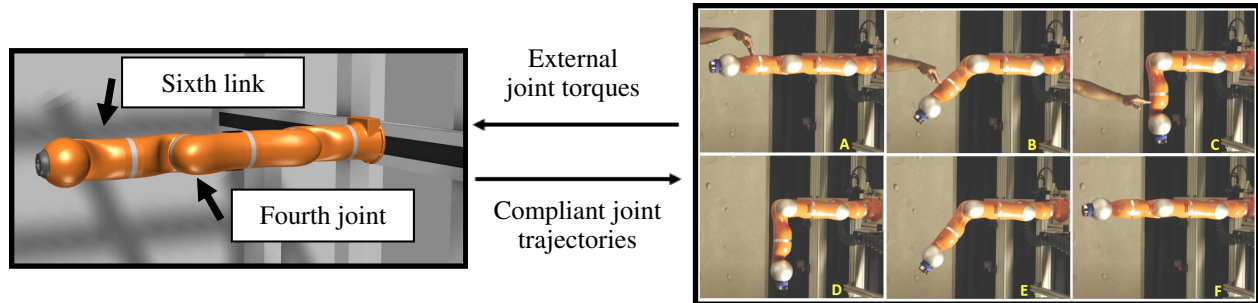


Figure 6. Experimental setup. Left: 3D simulation. Right: Real robot and interaction related to the first experiment.

was to move the fourth joint from its initial position  $q_4 = 0^\circ$  to the intermediate position  $q_4 = 90^\circ$  by interacting with the sixth link first. Then, the operator releases the link and the robot moves freely backwards to its initial configuration according to the chosen admittance parameters. The constant and variable admittance parameter cases were compared. As can be seen in Figure 7, constant admittance parameters give rise to a faster backwards joint motion when compared with the adapted parameters. The torque amplitude difference in Figure 8 (top) gives insight into the

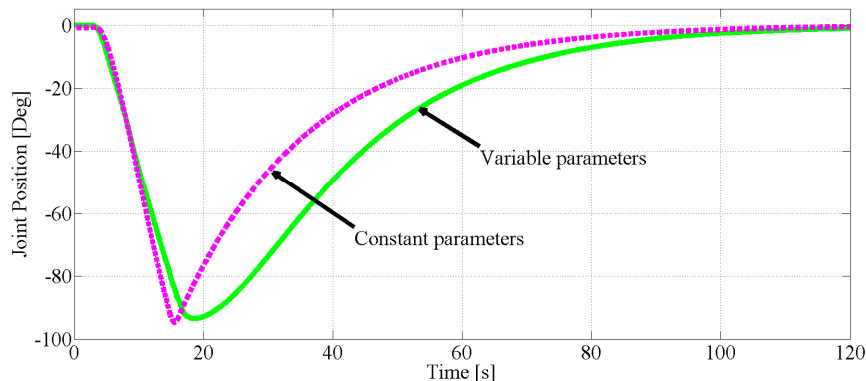


Figure 7. Real joint position during the first experiment.

amount of robot resistance felt during the interaction for the same angular deflection. It reveals that with adapted parameters the operator exerts considerably less external force in order to manually move the robot. This impression is confirmed in Figure 8 (bottom), which illustrates a measure for the deployed energy defined as the sum of the energy related to each joint (i.e. the product of real external torque and real joint velocity).

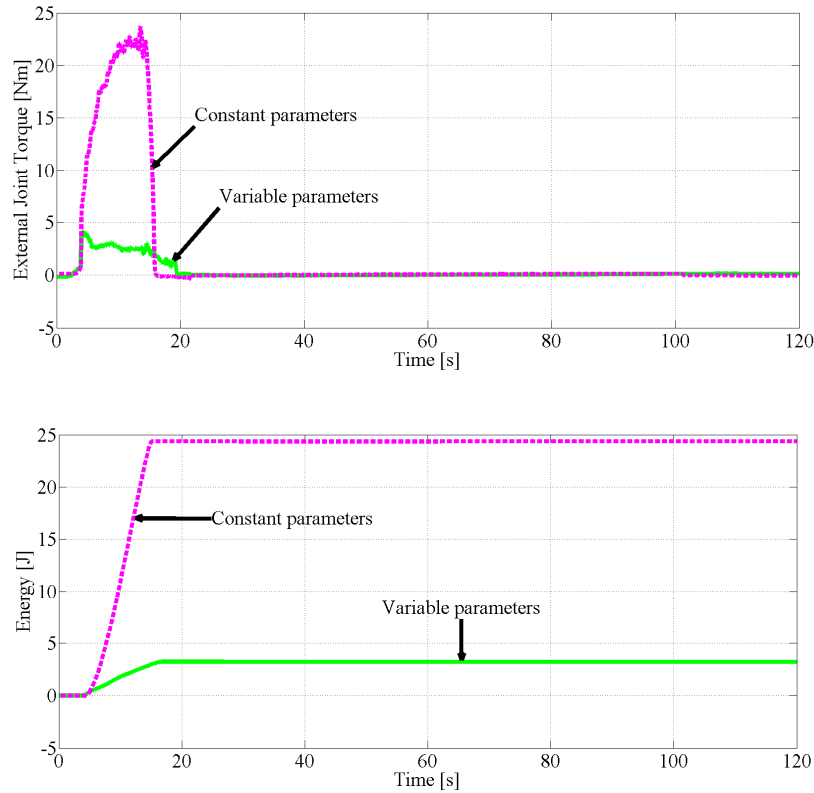


Figure 8. Top: Real external torque during interaction. Bottom: Energy deployed related to real robot.

## 5.2. EXPERIMENTS 2, 3 AND 4: ENHANCED, FULL BODY AND TCP-CENTERED GUIDANCE

A direct consequence of reducing the felt resistance is shown in Figure 9 (left hand side). The operator can move the otherwise rigidly behaving position-controlled robot by simply touching it with a finger. The guidance effort is substantially decreased. This capability is particularly useful in industrial manufacturing when it comes to being able to

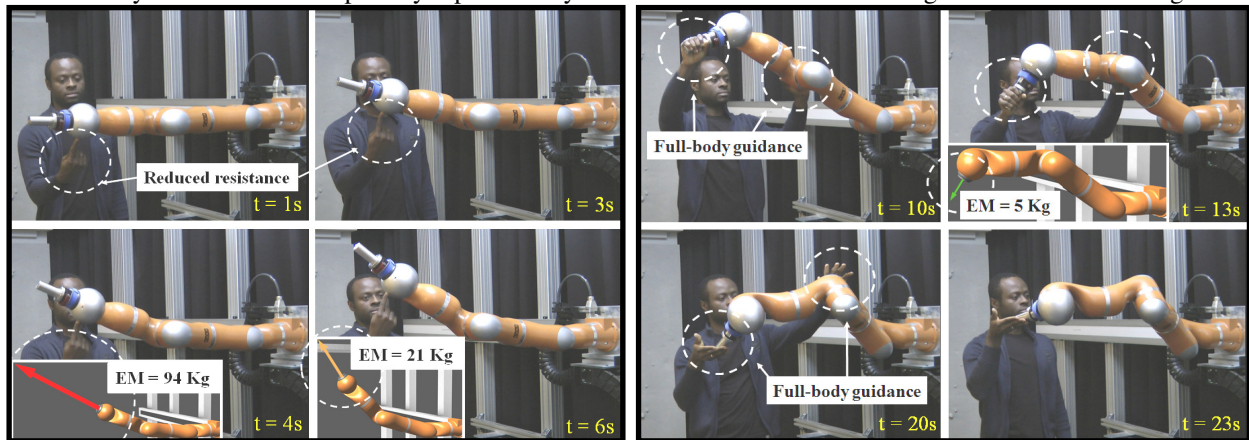


Figure 9. Left: Manipulation with reduced robot resistance. Right: Full body guidance. The encircled arrow is the effective mass.

easily carry heavy objects. It is worth to note that even though we explicitly make use of external torques as a means of communication between the operator and the robot to enable guidance, the simulated joint admittance control can be triggered by unwanted contacts as safety mode when no guidance is expected or a threshold torque limit is exceeded. This enhances safety in the robot workspace as the joint admittance absorbs the impact energy. Another way to improve safety along a given direction is to decrease the configuration- and dynamics-dependent effective mass along that direction [11]. Figure 9 (right hand side) shows how the current EM (computed and visualized on the simulator) decreases with human skills for optimization purposes in the loop. In addition, as shown in Figure 9 (right hand side), unlike current approaches that only focus on TCP guidance (see Figure 10), the operator can explicitly reach any desired posture compatible with kinematic constraints.

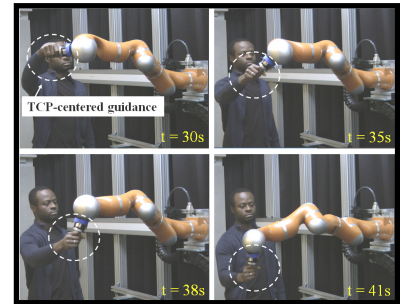


Figure 10. Guidance using end-link.

## 6. CONCLUSION

A 3D simulation-based approach for physical interactive robot guidance is presented in this paper. A dynamically simulated robot with joint admittance control capability is fed in real-time with real external joint torques. This leads to compliant joint trajectories that are fed back into the real controller to allow manual guidance. It is shown that adapting the admittance parameters substantially decreases the guidance effort and increases the ease of manipulation. Through full-body guidance the robot posture can be optimized with regard to the effective mass along a given direction. Together with the joint compliance this enhances safety in the robot workspace. The performance of the proposed approach is illustrated through several experiments on a physical 7 DoF robot manipulator. The approach offers new perspectives to position-controlled robot manipulators in manufacturing applications in terms of full-body manual guidance, safety assessment, task planning, 3D simulation-based functionalities extension and monitoring by using the symbiosis between robotics and virtual reality to enrich the guidance with useful information in real-time. This in turn highlights the effectiveness of eRobotics that laid the foundation on which this work has been developed.

## ACKNOWLEDGMENTS

The project IBOSS is funded by the German Aerospace Center (DLR) under grant number 50 RA 1203.

## REFERENCES

- [1] R. Balasubramanian, L. Xu, P. Brook, J.R. Smith, and Y. Matsuoka, "Physical Human Interactive Guidance: Identifying Grasping Principles from Human-Planned Grasps" *Robotics, IEEE Transactions on*, 28(4), 899–910, 2012
- [2] D. Colombo, D. Dallefrate, and L. Tosatti, "PC based control systems for compliance control and intuitive programming of industrial robots", *VDI Berichte, Volume 1956, Page 91*, 2006
- [3] M. Erden and J. Jonkman, "Physical Human-Robot Interaction by Observing Actuator Currents", *International Journal of Robotics and Automation, Volume 27, pages 233*, 2012
- [4] G. Ferretti, G. Magnani and P. Rocco, "Assigning virtual tool dynamics to an industrial robot through an admittance controller" *IEEE International conference on advanced robotics*, pages 1–6, 2009
- [5] J. Rossmann, M. Schluse, C. Schlette, and R. Waspe, "Control by 3D Simulation—A New eRobotics Approach to Control Design in Automation" *In Intelligent Robotics and Applications (pp. 186–197). Springer Berlin Heidelberg*, 2012
- [6] E. Guiffo Kaigom, T. J. Jung, and J. Rossmann, "Optimal Motion Planning of a Space Robot with Base Disturbance Minimization" *In 11th Symposium on Advanced Space Technologies in Robotics and Automation (pp. 1–6), ESA*, 2011
- [7] E. Guiffo Kaigom and J. Rossmann, "A new eRobotics approach: Simulation of adaptable joint admittance control", *In Mechatronics and Automation (ICMA), 2013 IEEE International Conference on (pp. 550–555). IEEE. Takamatsu, Japan*, 2013
- [8] J. Rossmann, "eRobotics: The symbiosis of advanced robotics and virtual reality technologies," in *Proc. of ASME 2012 Intern. Design Engin. Techn. Conf. and Comp. DETC-CIE 2012, Chicago, USA, Vol.2 - Part B. ASME*, pp. 1395ff, 2012
- [9] T. J. Jung, "Verfahren der Mehrkörperdynamiksimulation als Grundlage realitätsnaher Virtueller Welten", *PhD Dissertation, RWTH-Aachen University*, 2011
- [10] C. Ott, A. Albu-Schaffer, A. Kugi, and G. Hirzinger, "Decoupling based cartesian impedance control of flexible joint robots" *in Robotics and Automation, 2003. Proceedings. ICRA '03. IEEE International Conference on*, vol. 3. IEEE, pp. 3101–3107, 2003.
- [11] D. Shin, I. Sardellitti, Y.-L. Park, O. Khatib, and M. Cutkosky, "Design and control of a bio-inspired human-friendly robot," *The International Journal of Robotics Research*, vol. 29, no. 5, pp. 571–584, 2010